# Polarization of the $\Lambda^0$ Particle Produced from Protons in Carbon Nuclei by 1.17-BeV/$c$ Negative Pions*

YOUNG S. KIM†
*Department of Physics, Ohio State University, Columbus, Ohio*

AND

G. R. BURLESON,‡ P. I. P. KALMUS,§ A. ROBERTS, AND T. A. ROMANOWSKI§§
*Argonne National Laboratory, Argonne, Illinois*

(Received 4 August 1965)

The angular distribution of the direction and polarization of the $\Lambda^0$ particles produced from the protons in carbon nuclei by 1.17-BeV/$c$ $\pi^-$ have been measured in a magnetic-spark-chamber system. From a total of 794 observed $\Lambda^0$'s the mean polarization was found to be $-0.68\pm0.10$. Both the direction and polarization distributions show close similarity to those produced in hydrogen at this momentum.

## INTRODUCTION

DURING 1961–2 a group of Argonne physicists carried out, as guests of CERN, a series of runs at the CERN proton synchrotron with a large system of spark chambers in a magnetic field. In this first use of spark chambers for studying complex events, data were taken on interactions of 1.05–1.80 BeV/$c$ $\pi^-$ mesons in $CH_2$ and C targets. Descriptions of the apparatus and its performance have been published,[1–4] and a preliminary presentation of some results obtained in $\pi^0$ spectroscopy has been given.[5]

This paper presents the first analysis of some of our data on strange particle production, to wit, the angular distribution of polarization of $\Lambda^0$'s produced from the protons in carbon nuclei by 1.17-BeV/$c$ $\pi^-$. The analysis was motivated first by a need to study the carbon background in our measurements now in progress on the polarization of $\Sigma^0$'s produced in the $H_2$ content of a $CH_2$ target; and second, by the current absence of any satisfactory measurement of the polarization of the $\Lambda^0$'s produced in carbon.

## EXPERIMENTAL SETUP

The 44-ton magnet provided a working volume for spark chambers of dimensions 110×70×30 cm, and the experiment was run at a nominal field of 14 kG. The arrangement of spark chambers, target, counters, etc., inside the magnet is shown in Fig. 1.

The first two thin-plate chambers recorded the pions incident on a 1.4×1.5×8.0 cm target. The target (made of graphite in this experiment) was imbedded in a box of 6-mm thick scintillator, enclosing it on all sides except where the pions entered; the scintillator was used as an anticoincidence (AC) counter.

Several lead plates were included in the system to convert the gamma rays from $\Sigma^0$ decay. They had the adverse effect of markedly degrading the momentum accuracy obtainable for long tracks; long proton tracks were measured no more accurately than those ending at the first lead plate.

The chambers were made of etched aluminum plates averaging 25 mg/cm²; the part of the system between the target and the first lead plate, where most momentum measurements were made, included a total of about 0.75 g/cm² of Al and 0.6 g/cm² of scintillator, giving an effective radiation length of about 8 m.

Two views of the chamber, in 18° stereo, were separately recorded by Flight Research Model IV cameras on 35-mm film with a demagnification of 64:1.

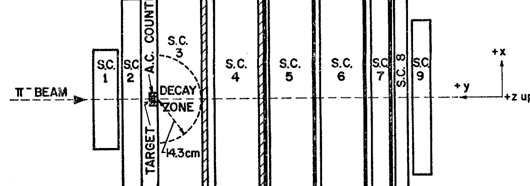


FIG. 1. Schematic diagram showing the spark-chamber arrangement. The whole assembly was inside a magnet; the $J$ and $H$ hodoscopes each included 8 scintillation counters.

* This work was performed on the proton synchrotron at CERN, Geneva, and was supported by CERN and the U. S. Atomic Energy Commission.

† Visiting Scientist at Argonne National Laboratory.

‡ Present address: Physics Department, Northwestern University, Evanston, Illinois.

§ Present address: Physics Department, Queen Mary College, London, England.

§§ Also at the Ohio State University, Columbus, Ohio.

[1] G. R. Burleson, J. A. DeShong, T. F. Hoang, P. I. P. Kalmus, R. L. Kuskowski, L. Q. Niemela, A. Roberts, T. A. Romanowski, S. D. Warshaw, and G. E. Yurka, Nucl. Instr. Methods **20**, 448 (1963).

[2] G. R. Burleson, T. F. Hoang, P. I. P. Kalmus, R. L. Kuskowski, L. Q. Niemela, A. Roberts, T. A. Romanowski, S. D. Warshaw, and G. E. Yurka, Nucl. Instr. Methods **20**, 180 (1963).

[3] G. R. Burleson, T. F. Hoang, P. I. P. Kalmus, R. L. Kuskowski, L. Q. Niemela, A. Roberts, T. A. Romanowski, S. D. Warshaw, and G. E. Yurka, Nucl. Instr. Methods **20**, 185 (1963).

[4] A. Roberts, in Proceedings of the International Symposium on Nuclear Electronics, Paris, 1963 (unpublished).

[5] G. R. Burleson, T. F. Hoang, P. I. P. Kalmus, L. Q. Niemela, A. Roberts, T. A. Romanowski, and S. D. Warshaw, Bull. Am. Phys. Soc. **9**, 69 (1964).

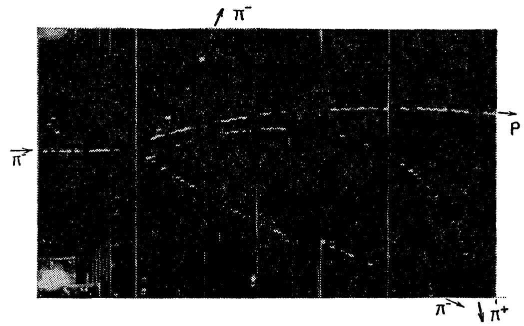


FIG. 2. A $K^0\Lambda^0$ associated production. Note that the proton track is brighter than the others.

Figure 2 shows an associated production event of the type reported in this paper.

The nominal beam momentum was $1.17\pm0.03$ BeV/$c$ at the entrance to the first chamber.[6]

The triggering logic is described in detail in Ref. 2. In brief, there was a threefold telescope (not shown) 1, 2, 3 in the incident pion beam; the anticoincidence box enclosing the target, 4; and two systems of eight hodoscope counters each, $J$ and $H$ (see Fig. 1). The required trigger was $123\bar{4}(2J2H$ or $3J1H)$, where $mJnH$ means any $m$ counters in $J$ and any $n$ in $H$. This "neutral trigger" requires that no charged particles leave the target and that at least two be observed in $J$ and one in $H$. At 1.17 BeV/$c$, this triggering arrangement, with a $CH_2$ target, yielded pictures of which more than half contained a $K^0$ or $\Lambda^0$, and about one-fifth showed both. The number of triggers was 50 per million incident pions.

The neutral trigger has the effect of almost completely suppressing events in which the $\Lambda^0$ is produced from a neutron in the carbon nucleus, since the observation of both $K^0$ and $\Lambda^0$ would require an additional $\pi^-$.

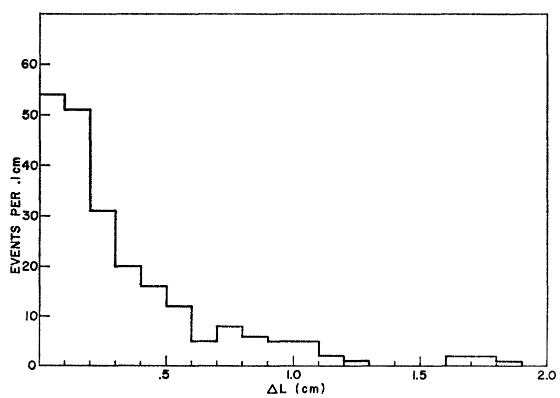


FIG. 3. Distribution of the vertex gap, i.e., the distance of the closest approach of the extrapolated lines of tracks forming the $V$. This is determined mainly by the coordinate measurement error along the nominal optic axis of the system.

[6] M. Barbier, J. D. Dowell, P. I. P. Kalmus, B. Leontic, A. Lundby, R. Meunier, G. Petrucci, L. Solinas, J. P. Stroot, and M. Szeptycka, Nucl. Instr. Methods **20**, 66 (1963).

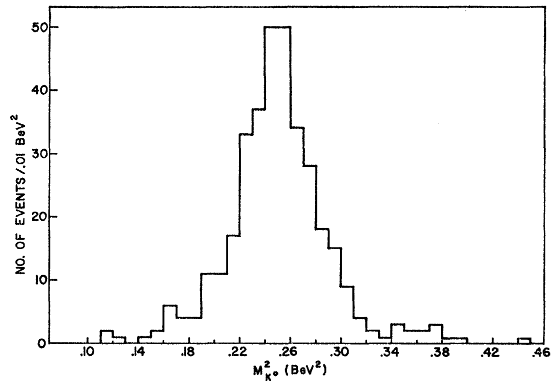


FIG. 4. Distribution of $K^0$-invariant mass squared.

## DATA ANALYSIS

The 20 000 pictures taken at 1.17 BeV/$c$ with a carbon target were triple-scanned for events that satisfied the following criteria:

(a) The event must have at least two $V$'s pointing back to the target.

(b) The apparent decay vertex must be within three gap-widths (3 cm) of the visible start of a paired track.

(c) There must be a beam track stopping in the target.

(d) A track must have at least two measurable sparks.

Measurers were instructed to measure the $\Lambda^0$ first. The identification is in most cases obvious at a glance from the heavier tracks produced by the proton from $\Lambda^0$ decay (see Fig. 2). The kinematics program GRIND verified the scanning assignment in about 90% of the cases.

Events accepted by scanners were measured on a SCAMP[7] image-plane digitizer which recorded the measurements on paper tape. A CDC-160A program rewrote the data on magnetic tape in the format required for the geometric reconstruction program.

A geometry program was required that provides spatial reconstruction of the points in space represented by the sparks, a least-squares fitting of these points to tracks, and an extrapolation of tracks to find vertices, which are not directly observable in narrow-gap chambers. Such a program, called TRAFIT,[8] was originally written. For the analysis of the present data, a revised version of TRAFIT, called GEOM, was prepared by one of us (YSK). The revised version provides an output data format suitable for introduction into the Argonne version of the CERN kinematics program GRIND.[9]

[7] J. A. DeShong, Jr., Rev. Sci. Instr. **33**, 859 (1962).

[8] TRAFIT was written by D. F. Carson, J. A. Gregory, R. J. Royston, and W. Snow.

[9] The Argonne version of GRIND is due to M. Appelbaum, K. Martin, and R. J. Royston.

GEOM locates decay vertices by finding the point of closest approach of the extrapolated pair of tracks forming the $V$. The distribution of the distance of closest approach (i.e., vertex gap) is given in Fig. 3. The median value is 2 mm. Because of the small-angle (18°) stereo-optics used, the minimum distance is determined primarily by the depth error.

GRIND examines paired tracks for fit to two single-vertex hypotheses: $\Lambda^0 \rightarrow \pi^- + p$ and $K^0 \rightarrow \pi^+ + \pi^-$. A good $V$ was required to satisfy one of these hypotheses with a $\chi^2$ probability greater than 0.01. Most rejected vertices were electron-positron pairs misidentified as $K^0$ or $\Lambda^0$ $V$'s. The scanners' identification on the basis of track density was used to resolve the $K^0\Lambda^0$ ambiguity, seen in about 10% of the accepted $K^0\Lambda^0$ pairs.

Figures 4 and 5 show the invariant mass distributions for $K^0$'s and $\Lambda^0$'s from $K^0\Lambda^0$ events, as computed from individual vertices using the unfitted variables. Any systematic error in the determination of momentum, or opening angle, would have shifted the peak from the expected point, as would also erroneous mass assignments by GRIND.

## ACCEPTANCE BIASES

A $K^0\Lambda^0$ pair was accepted only if both particles decayed inside a semicylindrical fiducial volume whose flat surface was defined by the $AC$ counter (see Fig. 1) and whose height was twice that of the target. The radius of the cylinder was 14.3 cm, the length of the "decay" chamber. For the $\Lambda^0$ angular distribution, each $K^0\Lambda^0$ pair was weighted by the inverse of its detection efficiency $\eta_K\eta_\Lambda$, where

$$\eta_\Lambda = \exp(-L_1/\gamma\beta c t_\Lambda) - \exp(-L_2/\gamma\beta c t_\Lambda), \qquad (1)$$

and $\eta_K$ is given by a similar equation. In Eq. (1) $L_1$ is the minimum distance the particle must travel before decaying to avoid the veto trigger, $L_2$ is the potential path length of the particle, $t_\Lambda$ is the $\Lambda^0$ lifetime at rest, and $\gamma\beta c$ has its conventional meaning and is calculated in the laboratory system. In obtaining $L_1$ and $L_2$, the production vertex was determined using the fitted $K^0$ and $\Lambda^0$ momenta. Events whose production vertex fell outside the target volume (about 5% of the total) were rejected. Figure 6 shows the resulting weighted angular distribution of the $\Lambda^0$ direction in the center of momentum system of the $K^0\Lambda^0$ pair. The solid curve represents the best fit to the cm angular distribution of $\Lambda^0$ produced in hydrogen by 1.17 BeV/$c$ negative pions.[10] The latter distribution has been normalized to least-square fit our data. If one assumes that the $\Sigma^0$ production angle distribution in carbon is like that in hydrogen, then the background $\Lambda^0$'s coming from $\Sigma^0$ decay will not alter appreciably our $\Lambda^0$ angular distribution, since the $\Sigma^0$ production angle distribution in our momentum range is very nearly isotropic as compared to the $\Lambda^0$ production angle distribution.[10,11]

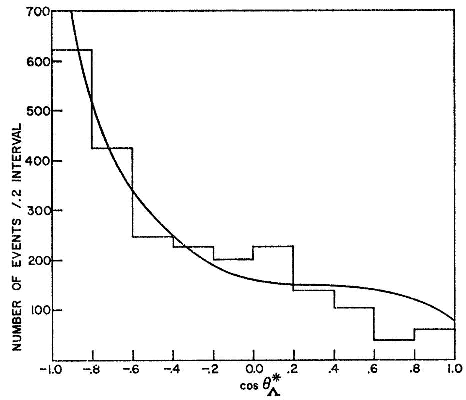


FIG. 6. Weighted angular distribution of $\Lambda^0$ in the $K^0\Lambda^0$ pair center-of-momentum system. The solid curve is a best fit to Anderson's hydrogen data at the same momentum.

The detection efficiency as given by Eq. (1) does not account for the following types of biases:

(a) A neutral particle may be "killed" even after emerging from the $AC$ counter, if one of its charged decay products flies backward into it.

(b) The hodoscope trigger requirement ($2J2H$ or $3J1H$) disfavors neutral particle decays where one charged particle carries away much of the available

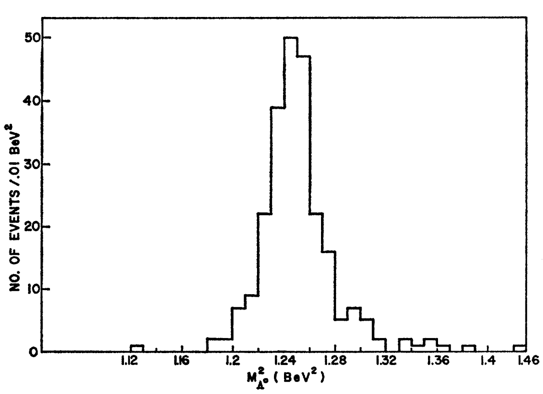


FIG. 5. Distribution of $\Lambda^0$-invariant mass squared.

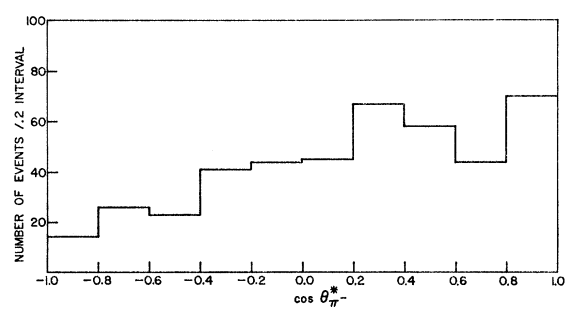


FIG. 7. Angular distribution of $\pi^-$ from $\Lambda^0$ decay with respect to $\Lambda^0$ line of flight in $\Lambda^0$ rest frame. The deviation from isotropy is due to detection biases.

[10] J. Anderson, UCRL-10838, 1963 (unpublished).
[11] J. Schwartz, UCRL-11360, 1964 (unpublished).

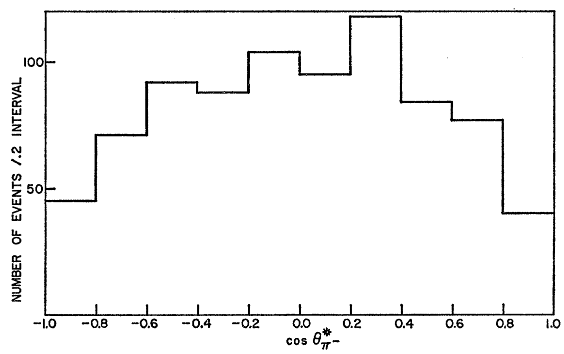


FIG. 8. Angular distribution of $\pi^-$ from $K^0$ decay with respect to the $K^0$ line of flight in $K^0$ rest frame. The deviation from isotropy is due to detection biases.

momentum and either leaves the other particle with insufficient rigidity to traverse the hodoscope counter or causes it to fly backward in the laboratory system.

(c) The hodoscope trigger requirement also disfavors neutral particle decays whose decay products traverse the same counter. (This bias is somewhat suppressed by the fiducial requirement.)

(d) The same requirement disfavors particles produced at large angles.

Bias (a) affects mainly low momentum and short-lived neutral particles, while bias (b) affects low momentum particles in general. The combined effects of these two biases plus the usual scanning bias against short tracks (tracks less than 3 gaps) are shown in the observed angular distribution of $\pi^-$ mesons from $\Lambda^0$ decay with respect to the $\Lambda^0$ line of flight evaluated in its rest frame (see Fig. 7). Figure 8 shows the effects of the same biases on the angular distribution of $\pi^-$ from $K^0$ decay with respect to the $K^0$ line of flight in its rest frame. The biases affect the distribution more or less symmetrically at the forward and backward angles, as expected from the $\pi^-\pi^+$ symmetry of the $K^0$ decay.

The main effect of biases (c) and (d) is that $\Lambda^0$'s produced at forward angles (laboratory) are seriously biased even at our beam momentum due to their associated $K^0$'s being either produced at large angles or with high momentum at forward angles (see Fig. 6).

The effect of these biases varies with the parameter measured. In $\Lambda^0$ polarization measurements, a bias that affects the angular distribution of $\Lambda^0$ is of no major consequence; it merely alters the number of events available for polarization analysis at any angular interval—provided, of course, that the polarization does not vary rapidly within the interval.

The type of bias most important in polarization measurements is any up-down asymmetry in the detection system with respect to any arbitrary production plane. This bias is minimized by the symmetry of the geometry with respect to any plane containing the incident pion path. To verify absence of any appreciable intrinsic asymmetry in our system, the up-down asymmetry of the $\pi^-$ from $K^0$ decay with respect the $K^0$ production plane in its rest frame was measured; but no significant asymmetry was observed, as shown in Fig. 9.

## RESULTS AND DISCUSSIONS

A total of 794 observed $K^0\Lambda^0$ pairs was divided into 8 bins according to the $\Lambda^0$ angle in the center-of-momentum system of the $K^0\Lambda^0$ pair, and for each bin, the $\Lambda^0$ polarization was obtained by maximizing the likelihood function

$$L(\alpha\langle\sigma(\theta)\rangle)=\prod_i(1+\alpha\langle\sigma(\theta)\rangle\mathbf{n}_i\cdot\mathbf{P}_\pi^*)\,, \qquad (2)$$

where $\alpha$ is the customary $\Lambda^0$ decay parameter, $\langle\sigma(\theta)\rangle$ is the polarization for $\Lambda^0$'s produced at the c.m. angle $\theta$. $\mathbf{n}$ is the unit vector normal to the $\Lambda^0$ production plane, and $\mathbf{P}_\pi^*$ is the unit vector along the decay pion momentum in the $\Lambda^0$ rest frame. The vector $\mathbf{n}$ was computed from the fitted $K^0$ and $\Lambda^0$ momenta using the expression $\mathbf{n}=\mathbf{P}_{K^0}\times\mathbf{P}_{\Lambda^0}/|\mathbf{P}_{K^0}\times\mathbf{P}_{\Lambda^0}|$. The average $\Lambda^0$ polarization was obtained by averaging $\langle\sigma(\theta)\rangle$ over the bins weighted according to the $\Lambda^0$ angular distribution in the $K^0\Lambda^0$ center-of-momentum system.

The variation of $\alpha\langle\sigma(\theta)\rangle$ with the $\Lambda^0$ angle in the $K^0\Lambda^0$ pair center-of-momentum system is shown in Fig.

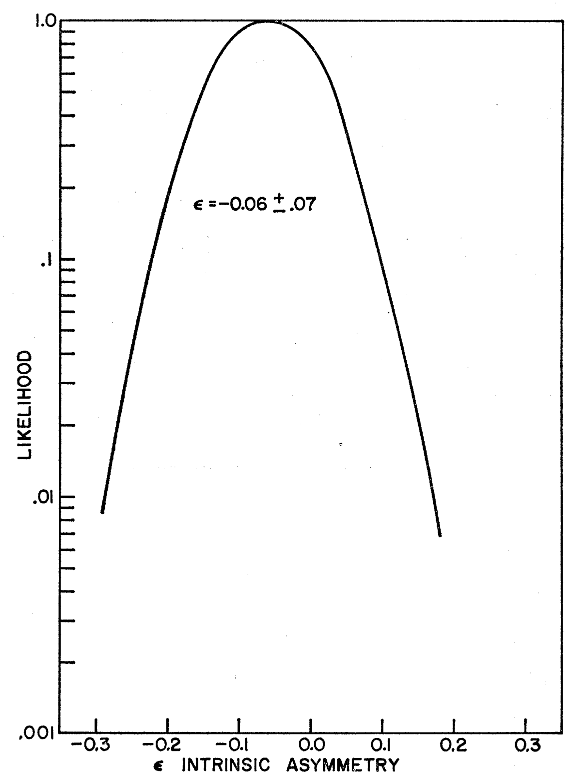


FIG. 9. Normalized likelihood function for the up-down asymmetry of the $\pi^-$ from $K^0$ decay with respect to the $K^0$ production plane. This asymmetry should be zero in the absence of bias in the polarization measurement.

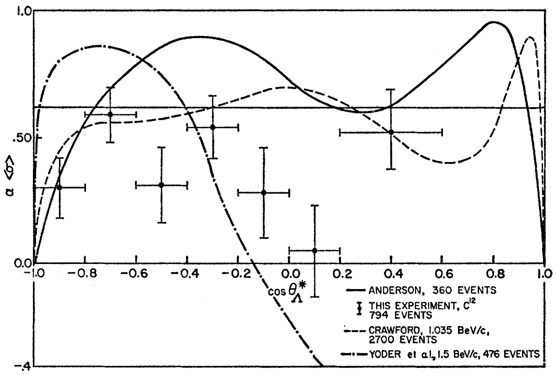


FIG. 10. Observed angular dependence of $\alpha\langle\sigma(\theta)\rangle$ of $\Lambda^0$'s from carbon. Note that the smooth curves represent hydrogen data at several beam momenta. Since $\alpha$ is $0.62\pm0.07$, the maximum possible value for $\alpha\langle\sigma\rangle$ is 0.62, corresponding to the horizontal line.

10. The solid curve is the best fit to the $\alpha\langle\sigma(\theta)\rangle$ data obtained by Anderson[8] for $\Lambda^0$'s produced in hydrogen by 1.17 BeV/$c$ pions. Anderson's data were obtained from 360 $\Lambda^0$'s and his statistical uncertainties are somewhat larger than ours. The $\Lambda^0$ polarization in carbon appears to be lower than Anderson's data especially near $\theta=90°$, but the difference is of questionable significance.

If one assumes that the impulse model approximation is valid for $K^0\Lambda^0$ production at our beam momentum, the difference between the carbon and hydrogen data can be explained qualitatively in terms of the Fermi momentum. The existing data on the variation of the polarization with $\pi^-$ beam momentum show that as the beam momentum increases, the $\Lambda^0$ polarization goes negative near $\theta=90°$ and then becomes positive near the forward direction.[11,12] Below 1.17 BeV/$c$, the polarization remains relatively high with its angular variation becoming small.[13]

That the observed $\Lambda^0$'s are produced predominantly through $\pi^-$ interaction with an individual proton without noticeably disturbing the residual nucleus (i.e., the impulse approximation) can be seen in Fig. 11 where the distribution of the effective target mass,

$$M_T=[(E_{K^0}+E_\Lambda-E_\pi)^2-(\mathbf{P}_{K^0}+\mathbf{P}_\Lambda-\mathbf{P}_\pi)^2]^{1/2}, \quad (3)$$

is shown. The width of the proton peak is consistent with our experimental resolution (~50 MeV). The events with lower effective target masses are non-two body $K^0\Lambda^0$ production events with one, or more, unobserved particle such as $K^0\Sigma^0(\Sigma^0\to\Lambda^0+\gamma)$ and $K^0\Lambda^0\pi^0$ events. Events in which the beam pion interacts with the nucleus as a whole tends to be rejected in our experiment because the star fragments trigger the $AC$ counter.

The average value of our $\alpha\langle\sigma\rangle$ over-all $\Lambda^0$ angles weighted with the $\Lambda^0$ angular distribution (see Fig. 6) is $0.42\pm0.04$ as compared to Anderson's value of $0.67\pm0.10$ obtained from $\Lambda^0$'s produced in hydrogen.[7] Other than the Fermi momentum described above, the difference between our average polarization and the hydrogen data may be due to several sources:

(a) Geometric bias. Since our triggering system was biased against low momentum (short life time), large angle $K^0$'s some of the $\Lambda^0$'s (which are highly polarized—see Fig. 10) associated with these $K^0$'s are not observed in our geometry (see Fig. 6). However, since these $\Lambda^0$'s constitute only about 2% of the total, the average $\Lambda^0$ polarization should be fairly independent of this bias.

(b) $\Sigma^0$ background. The fraction of $\Lambda^0$'s coming from non-two-body $K^0\Lambda^0$ production events may be estimated from the internal momentum distribution of nucleons in carbon and the distribution of the difference between the $K^0\Lambda^0$ pair momentum and the beam momentum $\Delta P=|\mathbf{P}_{K^0}+\mathbf{P}_\Lambda-\mathbf{P}_\pi|$. In Fig. 12, the solid curve represents the Fermi momentum distribution given in Ref. 14. The latter distribution has been normalized to fit the portion of the missing momentum histogram below $\Delta P=0.14$ BeV/$c$. The background thus obtained is about 30% of the total $\Lambda^0$'s observed. This figure is consistent with the available data on $K^0\Sigma^0$ and $K^0\Lambda^0$ production cross section in our momentum range.[10,11]

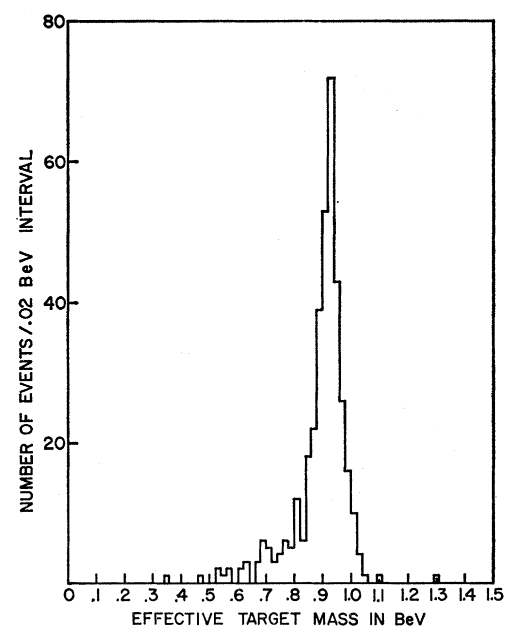


FIG. 11. Effective target mass for $K^0\Lambda^0$ production, calculated by assuming the mass target unknown and only $K^0$ and $\Lambda^0$ produced. The peak at the proton mass is about 50-MeV wide full width at half-maximum.

[12] L. L. Yoder, C. T. Coffin, D. I. Meyer, and K. M. Terwilliger, Phys. Rev. **132**, 1778 (1963).

[13] F. S. Crawford, in *Proceedings of the 1962 International Conference on High Energy Physics at CERN*, edited by J. Prentke (CERN, Geneva, 1962), p. 270.

[14] Y. S. Kim, Phys. Rev. **129**, 1293 (1963).

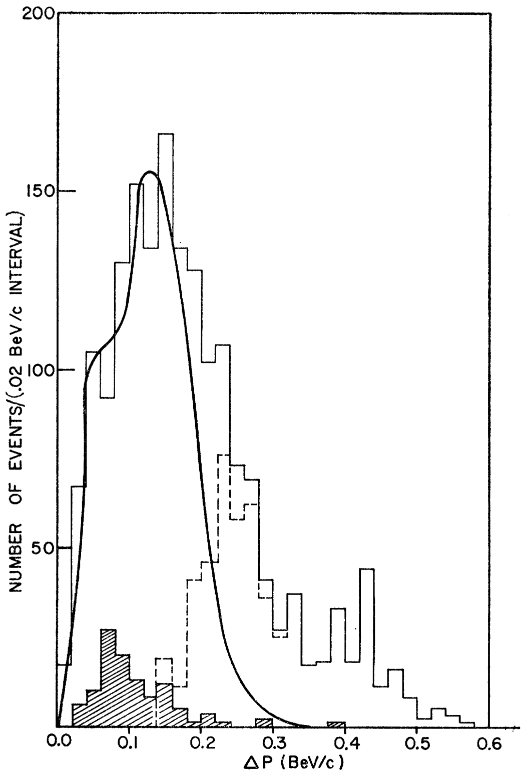


FIG. 12. Distribution of missing momentum,

$$\Delta P = |\mathbf{P}_{K^0} + \mathbf{P}_{\Lambda^0} - \mathbf{P}_{\pi^-}|.$$

The solid curve represents the expected Fermi momentum distribution given in Ref. 14. The pronounced difference between the solid curve and the histogram at large $\Delta P$ is due to $K^0\Sigma^0$ and $K^0\Lambda^0\pi^0$ events. The shaded area represents events which fit the kinematics of $K^0\Lambda^0$ production on free protons, and indicates the amount of background that would be introduced into measurements on hydrogen in a $CH_2$ target, for example. The dashed histogram (about 30% of the total area) represents the difference between the Fermi momentum distribution and our $\Delta P$ distribution and indicates the amount of $K^0\Sigma^0$ background.

The polarization of the $\Sigma^0$ particle produced by 1.17-BeV/$c$ $\pi^-$ particles in hydrogen is not yet well determined but is known to be consistent with zero.[10] Since the polarization of $\Lambda^0$'s from $\Sigma^0$ decay is on the average only one third of the $\Sigma^0$ polarization, the polarization error from this source is probably less than our statistical uncertainties.

(c) $\Lambda^0$-nucleon scattering. The total cross section for $\Lambda^0N$ elastic scattering at the mean $\Lambda^0$ momentum in this experiment (0.6 BeV/$c$) is about 10 mb as extrapolated from the existing data at lower momenta.[15–17] Using this figure and assuming the impulse approximation we estimate that about 16% of our $\Lambda^0$'s have suffered a scattering in the target. Fortunately, the existing data indicate that the $\Lambda^0N$ elastic scattering is predominantly forward-peaked and also, the $AC$ trigger would veto large angle scattering. Hence, the average depolarization of $\Lambda^0$'s due to scattering in the target should be very small as compared to our statistical uncertainties.

## CONCLUSION

We have measured the angular distribution of the polarization of the $\Lambda^0$ particles produced from protons in carbon by 1.17-BeV/$c$ pions. Using Cronin's[18] value of $\alpha = -0.62 \pm 0.07$, we obtain $\langle\sigma\rangle = -0.68 \pm 0.10$. This value is lower than Anderson's value ($-1.06 \pm 0.14$) for the polarization of the $\Lambda^0$ particles produced in $H_2$ by 1.17-BeV/$c$ $\pi^-$ mesons. This difference appears to be due mainly to the variation of the $\Lambda^0$ polarization with the $\pi^-$ beam momentum and the Fermi momentum distribution of the carbon protons.

## ACKNOWLEDGMENTS

We wish to thank Dr. John B. Adams (former CERN Director) and Professor G. Bernardini, who invited us to come to CERN; and Director V. F. Weisskopf and Professor P. Preiswek, who provided us assistance and the use of CERN facilities. We also thank the many people at CERN and Argonne who aided us in this project.

The Argonne group who participated in the data collection at CERN also included T. F. Hoang, L. Q. Niemela, and S. D. Warshaw, physicists; G. E. Yurka, R. L. Kustom, J. DeShong, R. Blumberg, and J. Terandy, engineers; and R. L. Pubentz, L. M. DeBall, H. C. Hollis, W. J. Evans, R. A. Martin, and B. H. Blair, technicians. Our special thanks are due to R. L. Buchleitner, S. R. McKissack, and S. M. O'Riordan for their most conscientious scanning and measuring efforts.

Finally, one of us (YSK) wishes to thank the Ohio State University for a grant of one year's research leave.

[15] B. Sechi-Zorn, R. A. Burnstein, T. B. Day, B. Kehoe, and G. A. Snow, Phys. Rev. Letters **13**, 282 (1964).
[16] T. H. Groves, Phys. Rev. **129**, 1372 (1963).
[17] L. Piekenbrock and F. Oppenheimer, Phys. Rev. Letters **12**, 625 (1964).
[18] J. W. Cronin and O. E. Overseth, Phys. Rev. **129**, 1795 (1963).

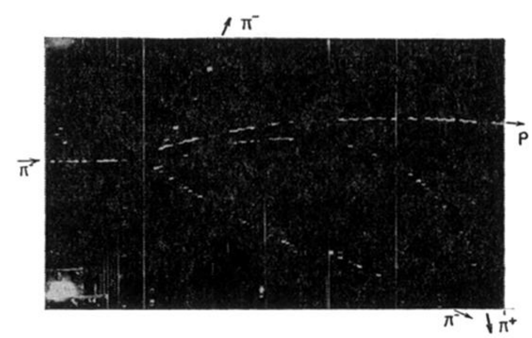


FIG. 2. A $K^0\Lambda^0$ associated production. Note that the proton track is brighter than the others.